JACS
JOURNAL OF THE AMERICAN CHEMICAL SOCIETY
pubs.acs.org/JACS
Article

Quantum Nuclear Dynamics on a Distributed Set of Ion-Trap Quantum Computing Systems

Anurag Dwivedi, A. J. Rasmusson, Philip Richerme, and Srinivasan S. Iyengar*

Cite This: https://doi.org/10.1021/jacs.4c07670
Read Online

ABSTRACT: Quantum nuclear dynamics with wavepacket time evolution is classically intractable and viewed as a promising avenue for quantum information processing. Here, we use IonQ, Inc.'s 11-qubit trapped-ion quantum computer, Harmony, to study the quantum wavepacket dynamics of a shared-proton within a short-strong hydrogen-bonded system. We also provide the first application of distributed quantum computing for chemical dynamics problems, where a distributed set of quantum processes is constructed using a tensor network formalism. For a range of initial states, we experimentally drive the ion-trap system to emulate the quantum nuclear wavepacket as it evolves along the potential surface generated from the electronic structure. Following the experimental creation of the nuclear wavepacket, we extract measurement observables such as its time-dependent spatial projection and its characteristic vibrational frequencies to good agreement with classical results. Vibrational eigenenergies obtained from quantum computation are in agreement with those obtained from classical simulations to within a fraction of a kilocalorie per mole, thus suggesting chemical accuracy. Our approach opens a new paradigm for studying the quantum chemical dynamics and vibrational spectra of molecules and also provides the first demonstration of parallel quantum computation on a distributed set of ion-trap quantum computers.

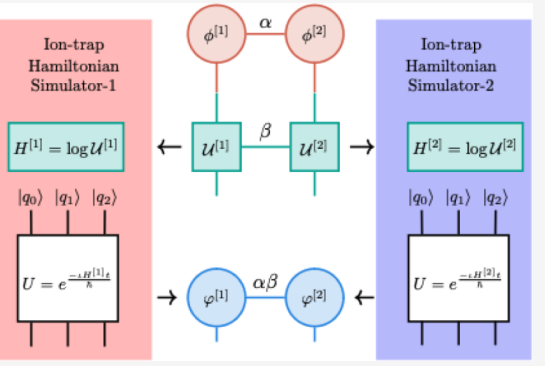

1. INTRODUCTION

Quantum nuclear dynamics has a critical impact on a range of problems of interest in biological, materials, and atmospheric systems. For example, the rate-limiting step in the oxidation of fatty acids by the enzyme, soybean lipoxygenase-1, is a hydrogen transfer step that is thought to be deeply impacted by quantum mechanical tunneling.[1−4] Protonated and hydroxide-rich water clusters that are thought to catalyze atmospheric reactions and are also of fundamental interest in condensed phase chemistry[5−7] have spectral features influenced by the quantum mechanical nature of the hydrated proton.[8−11] Several problems in materials chemistry including the study of nitrogen fixation[12−14] and artificial photosynthesis[15] are strongly controlled by such hydrogen transfer processes.[1] In all of these cases, there is a critical interplay between the electronic and nuclear degrees of freedom that influences chemical properties including reactivity.

The quantum chemical reaction dynamical study[16−48] of such complex problems entails the ab initio investigation of the time evolution of nuclear wavepackets on carefully constructed multidimensional potential energy surfaces (PES). The study of these problems leads naturally to detailed examination of chemical reaction dynamics and is considered to be an exponential scaling problem with nuclear dimension.[16,49−52] Indeed, such studies are deeply confounded by the following primary challenges: (a) Accurate electron correlation methods to compute PES have computational scaling[52] that is steeply algebraic,[53] where, for example, the well-known and extremely accurate CCSD(T) approach[54] scales as $O(N^{6-7})$ for N electrons in the system. (b) Quantum nuclear dynamics is, as noted above, thought to scale in an exponential manner with the increasing number of nuclear degree of freedom.[16,39,49−51,53−57]

This paper deals with the development of quantum algorithms for the study of quantum nuclear wavepacket dynamics and implementation of these ion quantum hardware. Our work here follows on our previous studies of quantum nuclear wavepacket dynamics on ion-trap systems[58,59] and provides one approach to extend these ideas to multidimensional quantum dynamics. While the implementation here is conducted on an ion-trap quantum hardware device, our algorithm is agnostic to hardware implementations and is in fact designed in such a way that it can be implemented on an ensemble of multiple kinds of quantum hardware systems. We perform our ion-trap experiments here on IonQ's 11-qubit trapped-ion quantum computer, Harmony. Our focus here is

Received: June 6, 2024
Revised: October 3, 2024
Accepted: October 4, 2024

on obtaining the vibrational properties, beyond the harmonic approximation, for specifically chosen nuclear degrees of freedom in a hydrogen-bonded system, through the simulation of the time evolution of a quantum nuclear wavepacket on an ion-trap quantum device.

We build on ref. 58, where we chose a single hydrogen-bonded system, with the hydrogen-bonded direction as the quantum mechanical degree of freedom (that is, one-dimensional quantum system), and this quantized dimension was directly treated on a Sandia National lab's, QSCOUT ion-trap quantum computer.[58] Good agreement was found between the classically studied wavepacket dynamics problem and that studied for the ion-trap quantum system. In contrast, here, not only do we provide a natural generalization of this application to more quantum nuclear dimensions, but also we provide a circuit-based implementation on a distributed set of ion-trap quantum computing systems, thus opening the doors for parallel quantum computation. Given that we are in the NISQ era of quantum computing,[102,103] with deep quantum circuits yielding large errors in computation, a distributed approach substantially reduces the circuit depth for these quantum operations and also provides a first parallel implementation of a chemical dynamics problem on quantum computers.

The specific problem of choice is a two-dimensional hydrogen-bonded system where, for simplicity, the hydrogen bond coordinate and a specific gating mode, which modulates the strength of the hydrogen bond, are together treated as a single two-dimensional quantum mechanical wavepacket. The evolution of this system is studied by using an ion-trap quantum computer. At the end, we find that the molecular vibrations captured from the time evolution of the wavepacket are in good agreement with quantum wavepacket dynamics studies on a classical computer. Our work complements other recent developments, including quantum simulations of vibronic spectra,[60−63] study of model potentials at conical intersections,[64−67] and algorithms for reduced dimensional reactive scattering studies.[68,69] Additionally, our work will greatly benefit from state-of-the-art algorithms for electronic structure[70−97] and their implementation on quantum hardware.[78,81,85,98−101]

2. METHODS

Our nuclear Hamiltonian comprises the nuclear kinetic energy operator and the multidimensional potential energy surface obtained from electronic structure calculations (for more details about the nuclear Hamiltonian, please refer to Supporting Information). The initial quantum nuclear wavepacket state is chosen as a matrix product state (MPS), where the quantum state is expressed as a tensor product of lower-rank tensors, each of which pertains to the individual physical dimensions of the nuclear vibrational problem. Figure 1 complements our discussion, and more details, including generalization to Figure 1, can be found in Supporting Information. The matrix product state for the initial wavepacket is represented as orange circles at the top of Figure 1a with entanglement, or bond, dimension α. This is a critical step here, as we will see in arriving at a distributed quantum computing protocol. Concurrently, the time-evolution operator is concisely represented in Figure 1a (green boxes) with entanglement, or bond, dimension β. Given that the time-evolution operator here arrives from electronic structure, this is further written out using the kinetic and electronic structure-based potential operators, as a Trotter factorization[104] in Figure 1b. Additionally, in Figure 1b, the potential propagator is also represented as a matrix product state, yielding for example, $\{\mathcal{V}^{[1]}\}$; $\{\mathcal{V}^{[2]}\}$, with bond dimensions β. The bond dimensions signify the extent of

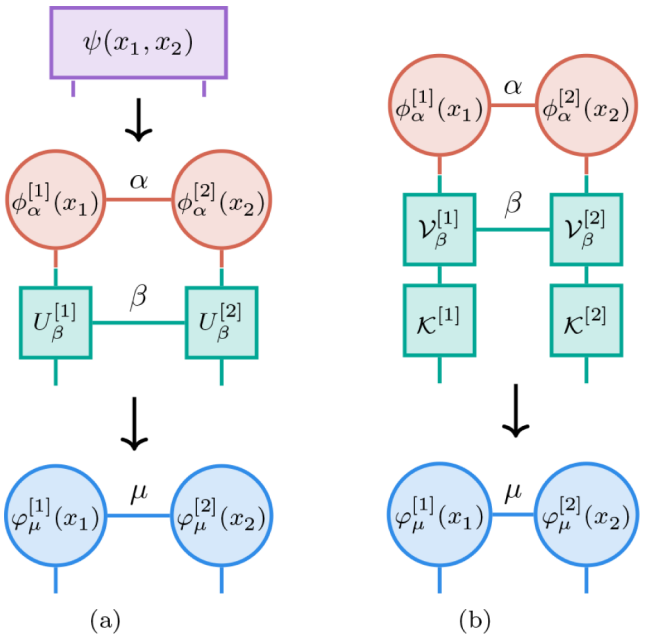

Figure 1. Figure 1a depicts the time evolution of the tensor network representation of a wavepacket. Figure 1b enumerates this action when the time evolution is written in Trotterized form. Here, the initial vector is given by entanglement variables α, while the Trotterized propagator has entangled variables β, which combine to determine the index $\mu = \alpha \times \beta$ for the propagated system.

entanglement or the number of such one-dimensional propagators and serve directly in creating quantum replicas to be processed on a distributed architecture. The final number of bond dimensions, that is $\alpha \times \beta$, is explicitly written out in Figure 1a, at the bottom, and is concisely represented as μ in Figure 1b.

Classically, we follow a procedure similar to that illustrated in Figure 1b, which involves the parallel application of one-dimensional potential propagators on each matrix product state (MPS) dimension. That is, the equivalent of $U_\beta^{[i]}\phi_\alpha^{[i]}(x_i) \rightarrow \varphi_{\alpha,\beta}^{[i]}(x_i)$. In this article, we examine a general quantum approach for such higher dimension problems, and this is described in Figure 2 with more details in Figure

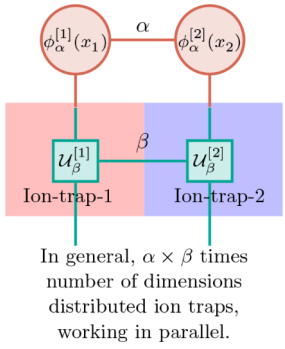

Figure 2. Derived from Figure 1a and depicting the simultaneous study of quantum dynamics for individual one-dimensional wave functions on distinct ion-trap quantum computers.

3 (also see Supporting Information where higher-dimensional generalizations are presented) As can be seen from Figure 2, we may create $\alpha \times \beta$ copies of unitary evolutions per dimension, each conducted on a different quantum hardware device. How this works in practice is shown in Figure 3. From each one-dimensional potential propagator ($\mathcal{V}_\beta^{[j]}$), we recover a one-dimensional potential and

https://doi.org/10.1021/jacs.4c07670
J. Am. Chem. Soc. XXXX, XXX, XXX−XXX

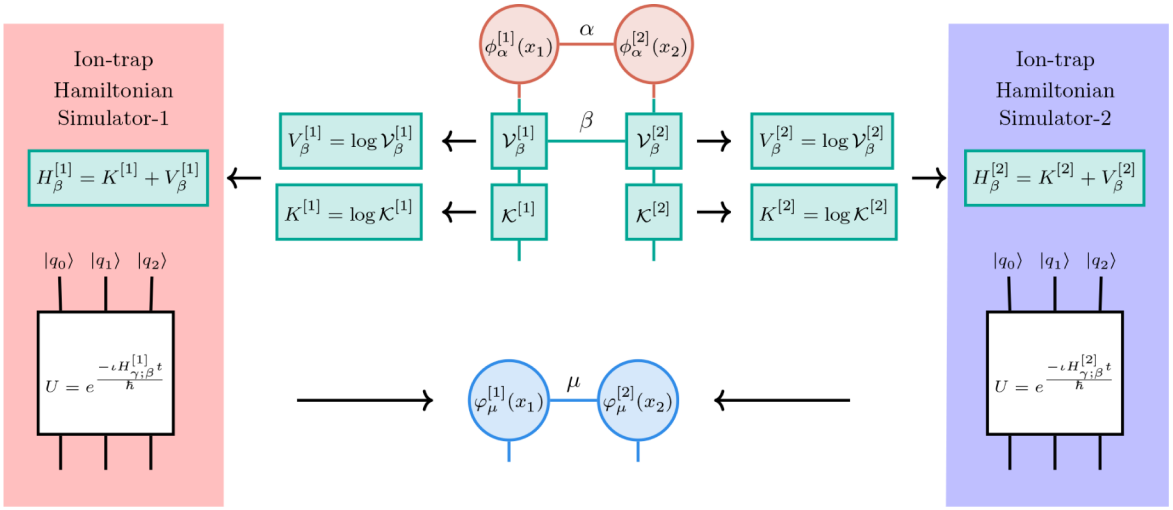

Figure 3. A detailed exposition of Figure 1a that precisely outlines how the distributed simulations are carried out. The individual one-dimensional potentials are derived from each one-dimensional propagator, as shown, yielding a family of effective one-dimensional Hamiltonians for the system. These individual one-dimensional Hamiltonians are then independently and concurrently simulated on separate ion-trap quantum computers.

construct Hamiltonians represented as $\{H_\beta^{[1]}\}$; $\{H_\beta^{[2]}\}$ in Figure 3, which now represent an array of separate one-dimensional quantum systems. These individual one-dimensional Hamiltonians are directly mapped onto separate ion-trap systems that individually propagate the different components of the entangled quantum system. The algorithm is hardware agnostic; hence, these individual one-dimensional Hamiltonians can also be simulated on an ensemble of a mixed set of quantum hardware systems. These aspects will be probed more in future publications.

Thus, in higher dimensions, each physical dimension would be independently propagated on distinct ion-trap quantum computers. The victory here comes from the following fact. It is well-known that, for correlated systems, as dimensionality increases, the quantum circuit depth of a general unitary goes exponential. For example, for an n-qubit unitary, one has a single 2^n by 2^n unitary operator, and a quantum circuit may, in general, require up to 4^n parameters. This exponential scaling poses a prohibitive challenge for computation, even in the quantum domain, let alone for the classical case. The current formalism, using the advantage of the MPS framework, may provide a family of separate quantum processes, studied independently, and the complexity of such processes grows as $2^{n_1} \times n_{\text{entangle}}$, where ${n_1}^{\mathcal{D}} = n$ for nuclear dimensionality $\mathcal{D}$. In some sense, the formalism here trades quantum circuit depth for quantum circuit breadth. Consequently, while the exponential scaling with nuclear dimensionality may be mitigated, there exists a linear scaling with the extent of entanglement n_{entangle} that may be present in the system. As chemistry tends to be local, the extent of entanglement is expected to scale as an area of the Hilbert space as per the area law of entanglement entropy, rather than the volume of the Hilbert space.[105−108] This results in a reasonable starting point for constructing an approximation for factored quantum dynamics on quantum computing platforms for higher dimensional problems.

Quantum computations are performed using IonQ's 11-qubit trapped-ion quantum computer, Harmony, and accessed through the cloud via Amazon Braket.[109,110] Each ion encodes an effective quantum bit with long coherence time and near-perfect state preparation and measurement.[109] Harmony's laser beam systems can separately address each ion, or pairs of ions, enabling arbitrary single-qubit gate rotations and all-to-all two-qubit gate connectivity. The wavepacket dynamics are simulated and measured on Harmony with 1000 repetitions for each time point. Quantum circuits (see Supporting Information) are executed in parallel such that the maximum number of qubits is in use during a computation.

3. RESULTS AND DISCUSSION

The system under investigation in this study is a bidentate-chelating agent known as 2,2′-bipyridine (see Figure 4). The

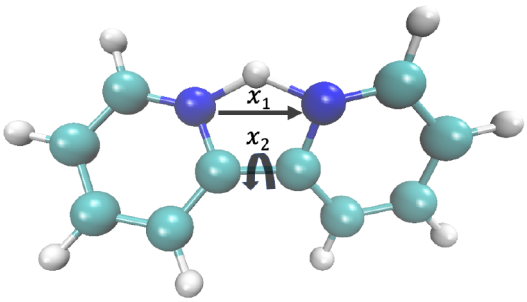

Figure 4. Protonated 2,2′-bipyridine system with the hydrogen bond dimension x_1 and gating dimension x_2 noted.

aromatic nitrogen-containing heterocycles within this molecule hold significance in a variety of applications, particularly in energy storage and catalytic oxidation.[111−113] Notably, the protonated form of 2,2′-bipyridine has garnered widespread attention due to its potential applications as both electron carriers and electron acceptors, while the deprotonated form serves as a potent chelating agent.[114,115]

The system depicted in Figure 4 is characterized by a shared proton stabilized through a N−H−N hydrogen bond. Furthermore, the ligand exhibits a structural arrangement featuring two planar pyridine rings interconnected by a carbon−carbon single bond, thus introducing a degree of torsional freedom. This torsional rotation of the C−C bond serves as a gating mode, regulating the spatial separation between the donor and acceptor atoms defining the hydrogen bond. Consequently, the torsional rotation of the C−C bond significantly influences the basicity or proton affinity of protonated 2,2′-bipyridine.[114] In this study, we focus on examining both the torsional angle (x_2) of the C−C bond and the corresponding relative proton position along the donor−acceptor axis, denoted as x_1, as illustrated in Figure 4.

In our scheme, the potential energy surface is computed through electronic structure methods, the details of which can

https://doi.org/10.1021/jacs.4c07670
J. Am. Chem. Soc. XXXX, XXX, XXX−XXX

be found in Supporting Information. The time evolution of this problem is studied classically, and to show that our quantum evaluation process works quite well, in Figures 5a−d, we

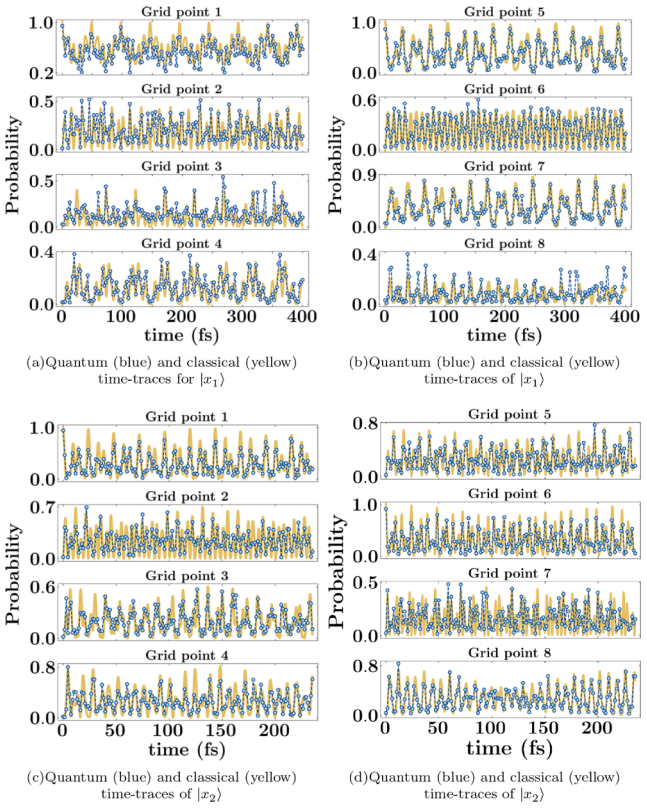

Figure 5. Illustrating the coherent dynamics of the wavepacket. The time evolution along specific grid points for the vibrational degree of freedom along the internuclear axis (x_1) connecting the two nitrogen atoms in Figure 4 is shown in parts (a,b). Figures (c,d) depict the quantum dynamics corresponding to the torsional degree of freedom (x_2) resulting from planar rotations of the pyridyl rings about the C−C bond. The projection of the wavepacket onto each grid point is shown separately. The left and right columns pertain to the two separate blocks of the Hamiltonian (see Supporting Information).

display the population of the time-evolved wavepackets on each grid basis state as for the classically treated and quantum mechanically treated problems. Due to the block diagonal nature of the Hamiltonian discussed in ref. 59 (see Supporting Information), each block of the Hamiltonian is simulated separately on two separate two-qubit ion-trap systems. Figure 5a,b shows the time traces of the upper and lower block diagonal Hamiltonian corresponding to the vibrational degree of freedom of the molecule (x_1) along the internuclear axis connecting two nitrogen nuclei, while Figure 5c,d depicts the time traces of the upper and lower block diagonal Hamiltonian corresponding to the torsional degree of freedom (x_2) resulting from planar rotations of the pyridyl rings about the C−C bond, respectively. The agreement between the quantum and classical calculations appears to be good but is gauged in further detail by probing the Fourier transforms of these time traces and comparing those with the respective eigenstates of the nuclear Hamiltonian.

In quantum mechanics, time correlations and their Fourier counterparts are generally used to probe expectation values. But as we discussed in ref. 58, and also in Supporting Information here, on quantum platforms, the individual terms within a correlation function become accessible to measurement. This provides us with another approach to compute these vibrational properties, which is done here, as was done in ref. 58. Specifically, vibrational properties are normally obtained from the Fourier transform of the density−density autocorrelation function. As can be seen in Supporting Information, inherently, there is a trace in all such observations as required by the expectation value that the fundamentals of quantum mechanics require us to perform. However, on a quantum computer, it is possible to measure the value of density at each basis point directly. Thus, in this publication, as in ref. 58, we have utilized this alternate formalism of computing vibrational properties that is not directly available through the Fourier transform of density−density autocorrelation function.

Along the same lines, in Figures 6 and 7, we present the experimentally derived frequency and energy spectra of protonated 2,2′-bipyridine, showcasing two distinct vibrational degrees of freedom. The first corresponds to the transfer of a proton along the internuclear axis (x_1) joining the two nitrogen atoms, while the second pertains to the torsional motion (x_2) associated with planar rotations of the pyridyl rings about the C−C bond. As mentioned earlier, leveraging the block-diagonal nature of the Hamiltonian (Supporting Information), each block is simulated separately on two distinct two-qubit ion-trap systems. The Fourier transformation corresponding to the upper and lower blocks of the Hamiltonian is depicted in panels a and b of Figures 6 and 7, respectively, corresponding to their respective degrees of freedom. Additionally, we compute the Fourier transform of the time evolution of the full Hamiltonian (see Supporting Information for theoretical details) to determine relative energy separations between the eigenstates of the respective blocks. In Figures 6 and 7, panel c illustrates the Fourier transform derived from the quantum dynamics of the full Hamiltonians. The meaning of the y-label in Figures 6 and 7a−c is described in detail in Supporting Information. Additionally, in panel d, frequencies extracted from panels a to c are color-coded according to their respective spectra, facilitating the experimental determination of relative energies for all eigenstates. Furthermore, panel e in Figures 6 and 7 presents a comparison between the energy eigenvalues from the quantum (represented by blue dots) and classical (depicted by dashed gray lines) simulations of the nuclear Hamiltonian corresponding to the respective degree of freedom.

At the end, from the Fourier transforms in Figures 6 and 7, we find all energy differences (Figure 8) between eigenvalues that populate a given initial state through our quantum computation on an ion-trap system. The accuracy of these eigenvalues is compared with that obtained from exact diagonalization. The absolute energy differences between the quantum-computed and those obtained from exact-diagonalization are shown in Figure 8. As can be seen, the mean absolute error is less than 0.2 kcal/mol, thus suggesting chemical accuracy. In a real chemical experiment, these eigenstates would be thermally populated, thus reducing the number of such eigenvalue differences found in accordance with the experiment, but here we find all eigenvalue differences within the initial wavepacket state. Finally, we utilize this information and find specific eigenstates from these eigenvalue differences, but already the agreement between eigenvalue differences classically computed and quantum computed is high.

https://doi.org/10.1021/jacs.4c07670
J. Am. Chem. Soc. XXXX, XXX, XXX−XXX

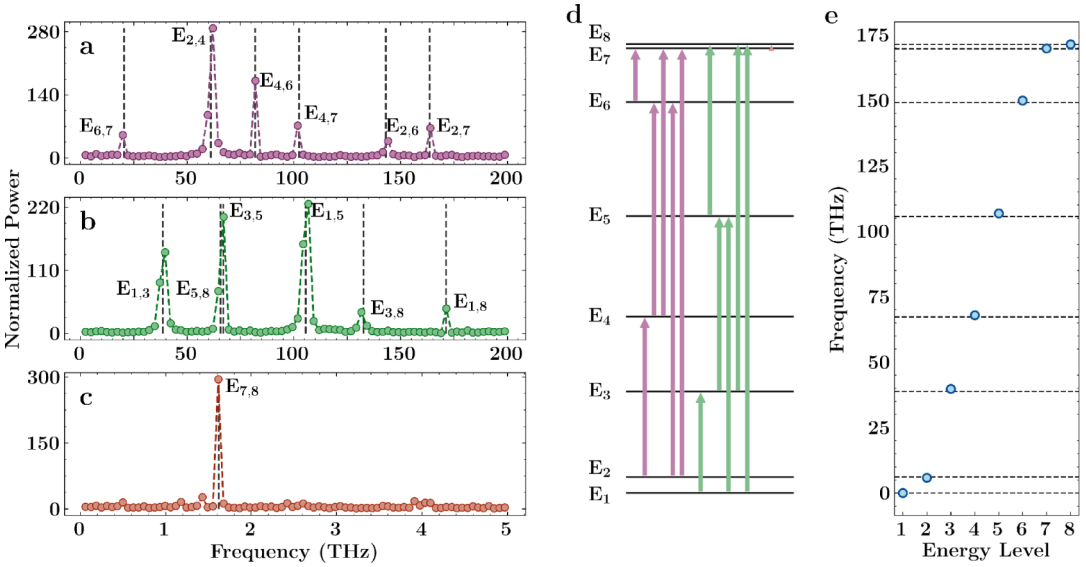

Figure 6. Figure presents the experimentally determined frequency and energy spectra of protonated 2,2′-bipyridine corresponding to the vibrational degree of freedom of transferring proton along the internuclear axis (x_1) joining the two nitrogen atoms. Due to the block diagonal nature of the Hamiltonian (see Supporting Information), each block of the Hamiltonian is simulated separately on two separate two-qubit ion-trap systems. The Fourier transform of the time evolution of the full-Hamiltonian (see Supporting Information for theoretical details) allows for the determination of relative energy separations between the eigenstates corresponding to the respective blocks. Panel (a) displays the cumulative Fourier transform obtained from the quantum propagation of the upper block with different initial wavepackets (more details in Supporting Information), while panel (b) illustrates the cumulative Fourier transform derived from the quantum propagation of the lower block of the Hamiltonian along the x_1-direction initialized with different wavepackets. Panel (c) shows the cumulative Fourier transform derived from the quantum dynamics of the full-Hamiltonian with two distinct initial wavepackets, providing the relative separation between the two sets of eigenstates corresponding to the lower and upper blocks. Figure 6d presents the extracted frequencies from panels (a−c), color-coded according to their parent spectrum. This presentation allows for the experimental determination of the relative energies of all eigenstates. Additionally, Figure 6e compares the quantum-computed energy eigenstates of the nuclear Hamiltonian (depicted as blue dots) with the results of exact diagonalization (shown as dashed gray lines).

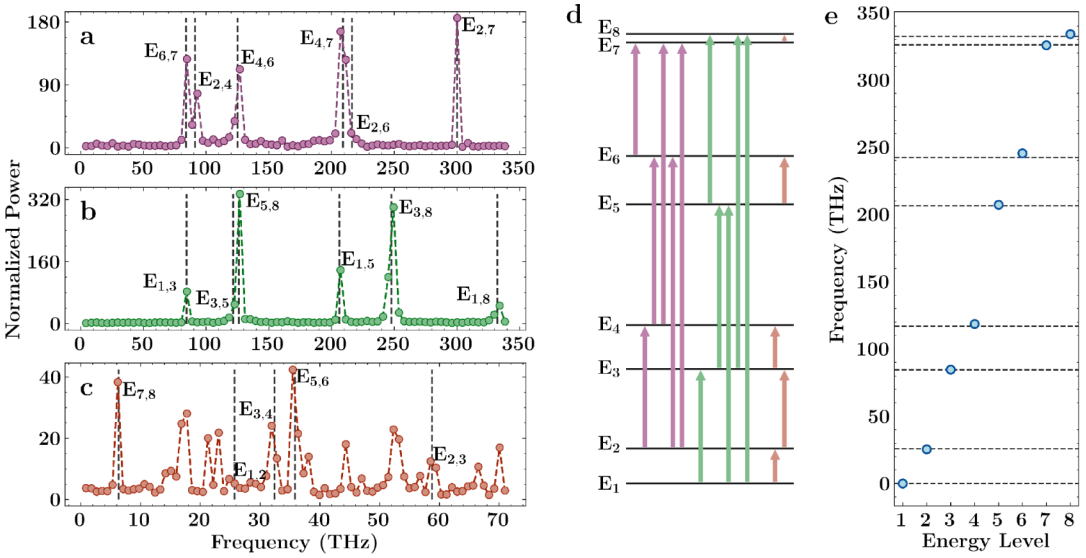

Figure 7. Figure presents the experimentally derived frequency and energy spectra of protonated 2,2′-bipyridine, focusing on the torsional degree of freedom (represented as x_2) associated with planar rotations of the pyridyl rings about the C−C bond. Leveraging the block diagonal structure of the Hamiltonian, each block is individually simulated by using separate two-qubit ion-trap systems. Panel (a) illustrates the cumulative Fourier transform resulting from quantum propagation of the upper block with 4 distict initial wavepackets (further details in Supporting Information), while panel (b) depicts the cumulative Fourier transform obtained from the quantum propagation of the lower block along the x_2-direction starting with different initial wavepackets. Panel (c) exhibits the Fourier transform derived from the quantum dynamics of the full-Hamiltonian, elucidating the relative separation between the eigenstates of the lower and upper blocks. Furthermore, in Figure 7d, frequencies extracted from panels (a−c) are color-coded by their respective spectra, facilitating the experimental determination of relative energies for all eigenstates. Additionally, Figure 7e presents a comparison between the quantum-computed energy eigenstates of the nuclear Hamiltonian (represented by blue dots) and exact diagonalization results (depicted by dashed gray lines).

https://doi.org/10.1021/jacs.4c07670
J. Am. Chem. Soc. XXXX, XXX, XXX−XXX

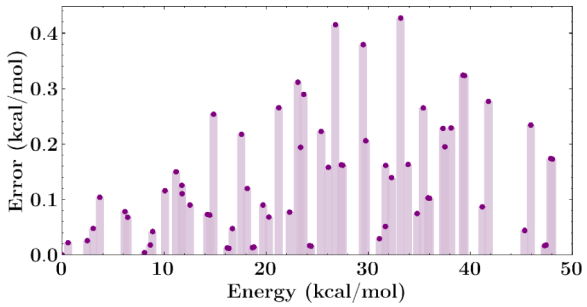

Figure 8. Mean absolute eigenenergy differences between the quantum computed and classically computed vibrational eigenenergies corresponding to the two chosen modes of protonated 2,2′-bipyridine. Information from Figures 6e and 7e is combined to form the vibrational energy spectrum. The mean absolute error between the quantum-computed energies and the exact-diagonalization results is 0.14 kcal/mol for first sixty-four energy levels.

4. CONCLUSIONS

In conjunction with the findings of ref. 58, we have demonstrated that quantum wavepacket dynamics studies can be constructed on ion-trap systems to good accuracy. While in ref. 58, the study is shown for a one-dimensional system, here, we have shown that this can be done for a hydrogen transfer mode that is coupled to a gating dimension. We also present a theory that readily generalizes to more-dimensional quantum dynamics problems. The complexity of the problem as given by the associated set of quantum circuits grows with the entanglement in the system. But we do not have an exponential scaling with dimension, and the circuit depth only grows in a proportional manner to the number of basis points used per dimension which may, in general, be fewer than the total number of dimensions in the problem. We believe that this approach offers a robust alternative to the challenges associated with quantum circuit depth and complexities in quantum nuclear dynamics.

■ ASSOCIATED CONTENT

Supporting Information

The Supporting Information is available free of charge at https://pubs.acs.org/doi/10.1021/jacs.4c07670.

A detailed overview of the theory for multidimensional quantum nuclear wavepacket dynamics, which is well-suited for implementation on distributed quantum systems. It also includes the potential energy surfaces used, experimental details, quantum circuit decomposition, and the time evolution using both classical and quantum hardware across a range of initial conditions; finally, it presents a comparison of the spectral features obtained from these simulations (PDF)

■ AUTHOR INFORMATION

Corresponding Author

Srinivasan S. Iyengar − *Department of Chemistry, Indiana University, Bloomington, Indiana 47405, United States; Indiana University Quantum Science and Engineering Center, Bloomington, Indiana 47405, United States;* orcid.org/0000-0001-6526-2907; Email: iyengar@indiana.edu

Authors

Anurag Dwivedi − *Department of Chemistry, Indiana University, Bloomington, Indiana 47405, United States; Indiana University Quantum Science and Engineering Center, Bloomington, Indiana 47405, United States*

A. J. Rasmusson − *Indiana University Quantum Science and Engineering Center, Bloomington, Indiana 47405, United States; Department of Physics, Indiana University, Bloomington, Indiana 47405, United States*

Philip Richerme − *Indiana University Quantum Science and Engineering Center, Bloomington, Indiana 47405, United States; Department of Physics, Indiana University, Bloomington, Indiana 47405, United States*

Complete contact information is available at: https://pubs.acs.org/10.1021/jacs.4c07670

Notes

The authors declare no competing financial interest.

■ ACKNOWLEDGMENTS

This work was supported by the U.S. National Science Foundation under awards OMA-1936353 and CHE-2311165 to SSI and PR and CHE-2102610 to SSI. The quantum computations were performed on IonQ's Harmony quantum computer through the IonQ Academic Research Credits Program to PR and SSI. AD acknowledges support from the John R. and Wendy L. Kindig Foundation.

■ REFERENCES

(1) Ludwig, R. *Hydrogen-Transfer Reactions* Hynes, J. T.; Klinman, J. P.; Limbach, H.-H.; Schowen, R. L., Eds.; Wiley-VCH: Weinheim, Germany, 2007.

(2) Klinman, J. P. Dynamically Achieved Active Site Precision in Enzyme Catalysis. *Acc. Chem. Res.* **2015**, *48*, 449−456.

(3) Hammes-Schiffer, S. Theory of Proton-Coupled Electron Transfer in Energy Conversion Processes. *Acc. Chem. Res.* **2009**, *42*, 1881−1889.

(4) Jonsson, T.; Glickman, M. H.; Sun, S. J.; Klinman, J. P. Experimental Evidence for Extensive Tunneling of Hydrogen in the Lipoxygenase Reaction: Implications for Enzyme Catalysis. *J. Am. Chem. Soc.* **1996**, *118*, 10319.

(5) Petersen, M. K.; Iyengar, S. S.; Day, T. J. F.; Voth, G. A. The Hydrated Proton at Water Liquid/Vapour Interfaces. *J. Phys. Chem. B* **2004**, *108*, 14804.

(6) Iyengar, S. S.; Day, T. J. F.; Voth, G. A. On the Amphiphilic Behavior of the Hydrated Proton: An *Ab Initio* Molecular Dynamics Study. *Int. J. Mass Spectrom.* **2005**, *241*, 197.

(7) Iyengar, S. S. Dynamical Effects on Vibrational and Electronic Spectra of Hydroperoxyl Radical Water Clusters. *J. Chem. Phys.* **2005**, *123*, 084310.

(8) Shin, J.-W.; Hammer, N. I.; Diken, E. G.; Johnson, M. A.; Walters, R. S.; Jaeger, T. D.; Duncan, M. A.; Christie, R. A.; Jordan, K. D. Infrared Signature of Structures Associated with the $H^+(H_2O)_n$ (N = 6 to 27) Clusters. *Science* **2004**, *304*, 1137.

(9) Headrick, J. M.; Diken, E. G.; Walters, R. S.; Hammer, N. I.; Christie, R. A.; Cui, J.; Myshakin, E. M.; Duncan, M. A.; Johnson, M. A.; Jordan, K. Spectral Signatures of Hydrated Proton Vibrations in Water Clusters. *Science* **2005**, *308*, 1765.

(10) Iyengar, S. S.; Petersen, M. K.; Day, T. J. F.; Burnham, C. J.; Teige, V. E.; Voth, G. A. The Properties of Ion-Water Clusters. I. the Protonated 21-Water Cluster. *J. Chem. Phys.* **2005**, *123*, 084309.

(11) Iyengar, S. S. Further Analysis of the Dynamically Averaged Vibrational Spectrum for the "magic" Protonated 21-Water Cluster. *J. Chem. Phys.* **2007**, *126*, 216101.

(12) Harris, D. F.; Lukoyanov, D. A.; Shaw, S.; Compton, P.; Tokmina-Lukaszewska, M.; Bothner, B.; Kelleher, N.; Dean, D. R.; Hoffman, B. M.; Seefeldt, L. C. The Mechanism of N_2 Reduction Catalyzed by Fe-Nitrogenase Involves Reductive Elimination of H_2. *Biochemistry* **2018**, *57*, 701−710.

(13) Thorneley, R. N. F.; Lowe, D. J. Kinetics and Mechanism of the Nitrogenase Enzymatic System. In *Molybdenum Enzymes*, Spiro, T. G., Ed.;Wiley: New York, 1985; Vol. *1*, pp. 221284.
(14) Yandulov, D. V.; Schrock, R. R. Reduction of Dinitrogen to Ammonia at a Well-Protected Reaction Site in a Molybdenum Triamidoamine Complex. *J. Am. Chem. Soc.* **2002**, *124*, 6252.
(15) Alstrum-Acevedo, J. H.; Brennaman, M. K.; Meyer, T. J. Chemical Approaches to Artificial Photosynthesis. 2. *Inorg. Chem.* **2005**, *44*, 6802.
(16) *Dynamics of Molecules and Chemical Reactions*; Wyatt, R. E.; Zhang, J. Z. H., Ed.; Marcel Dekker Inc.: New York NY, 1996.
(17) Bowman, J. M. The Self-Consistent-Field Approach to Polyatomic Vibrations. *Acc. Chem. Res.* **1986**, *19*, 202.
(18) McCoy, A. B.; Gerber, R. B.; Ratner, M. A. A Quantitative Approximation for the Quantum Dynamics of Hydrogen Transfer: Transition State Dynamics and Decay in $ClHCl^-$. *J. Chem. Phys.* **1994**, *101*, 1975.
(19) McCoy, A. B.; Huang, X.; Carter, S.; Bowman, J. M. Quantum studies of the vibrations in $H_3O_2^-$ and $D_3O_2^-$. *J. Chem. Phys.* **2005**, *123*, 064317.
(20) Iyengar, S. S.; Parker, G. A.; Kouri, D. J.; Hoffman, D. K. Symmetry-adapted distributed approximating functionals: Theory and application to the ro-vibrational states of H_3^+. *J. Chem. Phys.* **1999**, *110*, 10283−10298.
(21) Meyer, H.-D.; Manthe, U.; Cederbaum, L. S. The multi-configurational time-dependent Hartree approach. *Chem. Phys. Lett.* **1990**, *165*, 73−78.
(22) Lopreore, C. L.; Wyatt, R. E. Quantum Wave Packet Dynamics with Trajectories. *Phys. Rev. Lett.* **1999**, *82*, 5190.
(23) Schatz, G. C.; Kupperman, A. Quantum mechanical reactive scattering for three-dimensional atom plus diatom systems. I. Theory. *J. Chem. Phys.* **1976**, *65*, 4642−4667.
(24) Delos, J. B. Theory of Electronic Transitions in Slow Atomic Collisions. *Rev. Mod. Phys.* **1981**, *53*, 287.
(25) Feit, M. D.; Fleck, J. A. Solution of the Schrödinger Equation by a Spectral Method II: Vibrational Energy Levels of Triatomic Molecules. *J. Chem. Phys.* **1983**, *78*, 301.
(26) Feit, M. D.; Fleck, J. A., Jr Solution of the Schrödinger equation by a spectral method II: Vibrational energy levels of triatomic molecules. *J. Chem. Phys.* **1983**, *78*, 301−308.
(27) Feit, M. D.; Fleck, J. A., Jr Wave packet dynamics and chaos in the Hénon−Heiles system. *J. Chem. Phys.* **1984**, *80*, 2578.
(28) Kosloff, D.; Kosloff, R. A fourier method solution for the time dependent Schrödinger equation as a tool in molecular dynamics. *J. Comput. Phys.* **1983**, *52*, 35.
(29) Kosloff, D.; Kosloff, R. A Fourier method solution for the time dependent Schrödinger equation: A study of the reaction H++H2, D++HD, and D++H2. *J. Chem. Phys.* **1983**, *79*, 1823.
(30) Kosloff, R. Propagation Methods for Quantum Molecular Dynamics. *Annu. Rev. Phys. Chem.* **1994**, *45*, 145.
(31) Leforestier, C.; Bisseling, R. H.; Cerjan, C.; Feit, M. D.; Freisner, R.; Guldberg, A.; Hammerich, A.; Jolicard, D.; Karrlein, W.; Meyer, H. D.; et al. A Comparison of Different Propagation Schemes for the Time-Dependent Schrödinger Equation. *J. Comput. Phys.* **1991**, *94*, 59−80.
(32) DeVries, P. L. Fast Fourier Transform Techniques in Numerical Simulations of Intense Pulse-Molecule Interactions. In *Atomic and Molecular Processes with Short Intense Laser Pulses*. Bandrauk, A. D. Ed.; Springer: New York, 1988, Vol. *171*, p 481.
(33) Jang, H. W.; Light, J. C. Artificial Boundary Inhomogeneity Method for Quantum Scattering Solutions in an L^2 Basis. *J. Chem. Phys.* **1995**, *102*, 3262.
(34) Althorpe, S. C.; Clary, D. C. Quantum Scattering Calculations on Chemical Reactions. *Annu. Rev. Phys. Chem.* **2003**, *54*, 493.
(35) Althorpe, S. C.; Fernandez-Alonso, F.; Bean, B. D.; Ayers, J. D.; Pomerantz, A. E.; Zare, R. N.; Wrede, E. Observation and Interpretation of a Time-Delayed Mechanism in the Hydrogen Exchange Reaction. *Nature* **2002**, *416*, 67.
(36) Huang, Y.; Iyengar, S. S.; Kouri, D. J.; Hoffman, D. K. Further Analysis of Solutions to the Time-Independent Wavepacket Equations of Quantum Dynamics II: Scattering As a Continuous Function of Energy Using Finite, Discrete Approximate Hamiltonians. *J. Chem. Phys.* **1996**, *105*, 927.
(37) Miller, W. H.; Schwartz, S. D.; Tromp, J. W. Quantum Mechanical Rate Constants for Bimolecular Reactions. *J. Chem. Phys.* **1983**, *79*, 4889.
(38) Makri, N. Feynman Path Integration In Quantum Dynamics. *Comput. Phys. Commun.* **1991**, *63*, 389.
(39) Tal-Ezer, H.; Kosloff, R. An accurate and efficient scheme for propagating the time dependent Schrödinger equation. *J. Chem. Phys.* **1984**, *81*, 3967.
(40) Hartke, B.; Kosloff, R.; Ruhman, S. Large amplitude ground state vibrational coherence induced by impulsive absorption in CsI. A computer simulation. *Chem. Phys. Lett.* **1986**, *158*, 238−244.
(41) Iyengar, S. S.; Kouri, D. J.; Hoffman, D. K. Particular and Homogeneous Solutions of Time-Independent Wavepacket Schrodinger Equations: Calculations Using a Subset of Eigenstates of Undamped or Damped Hamiltonians. *Theor. Chem. Acc.* **2000**, *104*, 471.
(42) Lill, J. V.; Parker, G. A.; Light, J. C. Discrete Variable Representations and Sudden Models in Quantum Scattering-Theory. *Chem. Phys. Lett.* **1982**, *89*, 483.
(43) Light, J. C.; Hamilton, I. P.; Lill, J. V. J. Generalized discrete variable approximation in quantum mechanics. *Chem. Phys.* **1985**, *82*, 1400.
(44) Colbert, D. T.; Miller, W. H. A Novel Discrete Variable Representation for Quantum-Mechanical Reactive Scattering Via the S-Matrix Kohn Method. *J. Chem. Phys.* **1992**, *96*, 1982.
(45) Matsunaga, N.; Chaban, G. M.; Gerber, R. B. Degenerate perturbation theory corrections for the vibrational self-consistent field approximation: Method and applications. *J. Chem. Phys.* **2002**, *117*, 3541.
(46) Gerber, R.; Ratner, M. A. Self-consistent-field methods for vibrational excitations in polyatomic systems. In *Advances in Chemical Physics*, Prigogine, I.; Rice, S. A., Ed.; Wiley, 1988; Vol. *70*, p 97.
(47) Huang, Y.; Kouri, D. J.; Arnold, M.; Marchioro, T. L., II; Hoffman, D. K. Distributed Approximating Function Approach to Time-Dependent Wavepacket Propagation in 3-Dimensions: Atom-Surface Scattering. *Comput. Phys. Commun.* **1994**, *80*, 1−16.
(48) Jung, J. O.; Gerber, R. B. Vibrational wave functions and spectroscopy of $(H_2O)_n$, n = 2, 3, 4, 5: Vibrational self-consistent field with correlation corrections. *J. Chem. Phys.* **1996**, *105*, 10332.
(49) Feynman, R. P.; Hey, J.; Allen, R. W. *Feynman Lectures on Computation*; Addison-Wesley Longman Publishing Co., Inc, 1998.
(50) Nielsen, M. A.; Chuang, I. L. *Quantum computation and quantum information*; Cambridge University Press: Cambridge, 2000.
(51) Feynman, R. P. Simulating physics with computers. *Int. J. Theor. Phys.* **1982**, *21*, 467−488.
(52) Berman, L. The complexity of logical theories. *Theor. Comput. Sci.* **1980**, *11*, 71−77.
(53) Schlegel, H. B.; Frisch, M. J. Computational bottlenecks in molecular orbital calculations. In *Theoretical and Computational Models for Organic Chemistry*; Springer, 1991; pp. 533.
(54) Raghavachari, K.; Trucks, G. W.; Pople, J. A.; Head-Gordon, M. A fifth-order perturbation comparison of electron correlation theories. *Chem. Phys. Lett.* **1989**, *157*, 479−483.
(55) Deumens, E.; Diz, A.; Longo, R.; Öhrn, Y. Time-Dependent Theoretical Treatments of the Dynamics of Electrons and Nuclei in Molecular-Systems. *Rev. Mod. Phys.* **1994**, *66*, 917.
(56) Kuppermann, A. Wyatt, R. E.; Zhang, J. Z. H. The Geometric Phase in Reaction Dynamics. In *Dynamics of Molecules and Chemical Reactions*; Marcel Dekker Inc.: New York, NY, 1996; p 411
(57) Kouri, D. J.; Zhu, W.; Ma, X.; Pettitt, B. M.; Hoffman, D. K. Monte Carlo evaluation of real-time Feynman path integrals for quantal many-body dynamics: distributed approximating functions and Gaussian sampling. *J. Phys. Chem.* **1992**, *96*, 9622.

https://doi.org/10.1021/jacs.4c07670
J. Am. Chem. Soc. XXXX, XXX, XXX−XXX

(58) Richerme, P.; Revelle, M. C.; Yale, C. G.; Lobser, D.; Burch, A. D.; Clark, S. M.; Saha, D.; Lopez-Ruiz, M. A.; Dwivedi, A.; Smith, J. M.; et al. Quantum computation of hydrogen bond dynamics and vibrational spectra. *J. Phys. Chem. Lett.* **2023**, *14*, 7256−7263.
(59) Saha, D.; Iyengar, S. S.; Richerme, P.; Smith, J. M.; Sabry, A. Mapping Quantum Chemical Dynamics Problems to Spin-Lattice Simulators. *J. Chem. Theory Comput.* **2021**, *17*, 6713−6732.
(60) Sparrow, C.; Martín-López, E.; Maraviglia, N.; Neville, A.; Harrold, C.; Carolan, J.; Joglekar, Y. N.; Hashimoto, T.; Matsuda, N.; O'Brien, J. L.; Tew, D. P.; Laing, A. Simulating the vibrational quantum dynamics of molecules using photonics. *Nature* **2018**, *557*, 660−667.
(61) Wang, C. S.; Curtis, J. C.; Lester, B. J.; Zhang, Y.; Gao, Y. Y.; Freeze, J.; Batista, V. S.; Vaccaro, P. H.; Chuang, I. L.; Frunzio, L.; Jiang, L.; Girvin, S. M.; Schoelkopf, R. J. Efficient Multiphoton Sampling of Molecular Vibronic Spectra on a Superconducting Bosonic Processor. *Phys. Rev. X* **2020**, *10*, 021060.
(62) Huh, J.; Guerreschi, G. G.; Peropadre, B.; McClean, J. R.; Aspuru-Guzik, A. Boson sampling for molecular vibronic spectra. *Nat. Photonics* **2015**, *9*, 615−620.
(63) Wang, Y.; Sager-Smith, L. M.; Mazziotti, D. A. Quantum Simulation of Bosons with the Contracted Quantum Eigensolver. *New J. Phys.* **2023**, *25*, 103005.
(64) Wang, C. S.; Frattini, N. E.; Chapman, B. J.; Puri, S.; Girvin, S. M.; Devoret, M. H.; Schoelkopf, R. J. Observation of Wave-Packet Branching through an Engineered Conical Intersection. *Phys. Rev. X* **2023**, *13*, 011008.
(65) Valahu, C. H.; Olaya-Agudelo, V. C.; MacDonell, R. J.; Navickas, T.; Rao, A. D.; Millican, M. J.; Pérez-Sánchez, J. B.; Yuen-Zhou, J.; Biercuk, M. J.; Hempel, C.; et al. Direct observation of geometric-phase interference in dynamics around a conical intersection. *Nat. Chem.* **2023**, *15*, 1503−1508.
(66) Whitlow, J.; Jia, Z.; Wang, Y.; Fang, C.; Kim, J.; Brown, K. R. Quantum simulation of conical intersections using trapped ions. *Nat. Chem.* **2023**, *15*, 1509−1514.
(67) Wang, Y.; Mazziotti, D. A. Quantum simulation of conical intersections. *Phys. Chem. Chem. Phys.* **2024**, *26*, 11491−11497.
(68) Xing, X.; Gomez Cadavid, A.; Izmaylov, A. F.; Tscherbul, T. V. A hybrid quantum-classical algorithm for multichannel quantum scattering of atoms and molecules. *J. Phys. Chem. Lett.* **2023**, *14*, 6224−6233.
(69) Kale, S. S.; Kais, S. Simulation of Chemical Reactions on a Quantum Computer. *J. Phys. Chem. Lett.* **2024**, *15*, 5633−5642.
(70) Jordan, P.; Wigner, E. Über das Paulische Äquivalenzverbot. *Z. Phys.* **1928**, *47*, 631−651.
(71) Ortiz, G.; Gubernatis, J. E.; Knill, E.; Laflamme, R. Quantum algorithms for fermionic simulations. *Phys. Rev. A* **2001**, *64*, 022319.
(72) Bravyi, S. B.; Kitaev, A. Y. Fermionic Quantum Computation. *Ann. Phys.* **2002**, *298*, 210−226.
(73) Aspuru-Guzik, A.; Dutoi, A. D.; Love, P. J.; Head-Gordon, M. Simulated quantum computation of molecular energies. *Science* **2005**, *309*, 1704.
(74) Kirby, W. M.; Love, P. J. Variational Quantum Eigensolvers for Sparse Hamiltonians. *Phys. Rev. Lett.* **2021**, *127*, 110503.
(75) Cervera-Lierta, A.; Kottmann, J. S.; Aspuru-Guzik, A. Meta-Variational Quantum Eigensolver: Learning Energy Profiles of Parameterized Hamiltonians for Quantum Simulation. *PRX Quantum* **2021**, *2*, 020329.
(76) O'Malley, P. J. J.; Babbush, R.; Kivlichan, I. D.; Romero, J.; McClean, J. R.; Barends, R.; Kelly, J.; Roushan, P.; Tranter, A.; Ding, N.; Campbell, B.; Chen, Y.; Chen, Z.; Chiaro, B.; Dunsworth, A.; Fowler, A. G.; Jeffrey, E.; Lucero, E.; Megrant, A.; Mutus, J. Y.; Neeley, M.; Neill, C.; Quintana, C.; Sank, D.; Vainsencher, A.; Wenner, J.; White, T. C.; Coveney, P. V.; Love, P. J.; Neven, H.; Aspuru-Guzik, A.; Martinis, J. M. Scalable Quantum Simulation of Molecular Energies. *Phys. Rev. X* **2016**, *6*, 031007.
(77) Smart, S. E.; Mazziotti, D. A. Quantum Solver of Contracted Eigenvalue Equations for Scalable Molecular Simulations on Quantum Computing Devices. *Phys. Rev. Lett.* **2021**, *126*, 070504.
(78) Kandala, A.; Mezzacapo, A.; Temme, K.; Takita, M.; Brink, M.; Chow, J. M.; Gambetta, J. M. Hardware-efficient variational quantum eigensolver for small molecules and quantum magnets. *Nature* **2017**, *549*, 242.
(79) Xia, R.; Kais, S. Quantum machine learning for electronic structure calculations. *Nat. Commun.* **2018**, *9*, 4195.
(80) Gorman, D. J.; Hemmerling, B.; Megidish, E.; Moeller, S. A.; Schindler, P.; Sarovar, M.; Haeffner, H. Engineering vibrationally assisted energy transfer in a trapped-ion quantum simulator. *Phys. Rev. X* **2018**, *8*, 011038.
(81) Nam, Y.; Chen, J.-S.; Pisenti, N. C.; Wright, K.; Delaney, C.; Maslov, D.; Brown, K. R.; Allen, S.; Amini, J. M.; Apisdorf, J.; et al. Ground-state energy estimation of the water molecule on a trapped-ion quantum computer. *Npj Quantum Inf.* **2020**, *6*, 33.
(82) Wang, B.-X.; Tao, M.-J.; Ai, Q.; Xin, T.; Lambert, N.; Ruan, D.; Cheng, Y.-C.; Nori, F.; Deng, F.-G.; Long, G.-L. Efficient quantum simulation of photosynthetic light harvesting. *Npj Quantum Inf.* **2018**, *4*, 52.
(83) Chin, A. W.; Mangaud, E.; Atabek, O.; Desouter-Lecomte, M. Coherent quantum dynamics launched by incoherent relaxation in a quantum circuit simulator of a light-harvesting complex. *Phys. Rev. A* **2018**, *97*, 063823.
(84) Potočnik, A.; Bargerbos, A.; Schröder, F. A. Y. N.; Khan, S. A.; Collodo, M. C.; Gasparinetti, S.; Salathé, Y.; Creatore, C.; Eichler, C.; Türeci, H. E.; et al. Studying light-harvesting models with superconducting circuits. *Nat. Commun.* **2018**, *9*, 904.
(85) Peruzzo, A.; McClean, J.; Shadbolt, P.; Yung, M.-H.; Zhou, X.-Q.; Love, P. J.; Aspuru-Guzik, A.; O'brien, J. L. A variational eigenvalue solver on a photonic quantum processor. *Nat. Commun.* **2014**, *5*, 4213.
(86) Grimsley, H. R.; Economou, S. E.; Barnes, E.; Mayhall, N. J. An adaptive variational algorithm for exact molecular simulations on a quantum computer. *Nat. Commun.* **2019**, *10*, 3007.
(87) Arute, F.; Arya, K.; Babbush, R.; Bacon, D.; Bardin, J. C.; Barends, R.; Boixo, S.; Broughton, M.; Buckley, B. B.; Buell, D. A.; Burkett, B.; Bushnell, N.; Chen, Y.; Chen, Z.; Chiaro, B.; Collins, R.; Courtney, W.; Demura, S.; Dunsworth, A.; Farhi, E.; Fowler, A.; Foxen, B.; Gidney, C.; Giustina, M.; Graff, R.; Habegger, S.; Harrigan, M. P.; Ho, A.; Hong, S.; Huang, T.; Huggins, W. J.; Ioffe, L.; Isakov, S. V.; Jeffrey, E.; Jiang, Z.; Jones, C.; Kafri, D.; Kechedzhi, K.; Kelly, J.; Kim, S.; Klimov, P. V.; Korotkov, A.; Kostritsa, F.; Landhuis, D.; Laptev, P.; Lindmark, M.; Lucero, E.; Martin, O.; Martinis, J. M.; McClean, J. R.; McEwen, M.; Megrant, A.; Mi, X.; Mohseni, M.; Mruczkiewicz, W.; Mutus, J.; Naaman, O.; Neeley, M.; Neill, C.; Neven, H.; Niu, M. Y.; O'Brien, T. E.; Ostby, E.; Petukhov, A.; Putterman, H.; Quintana, C.; Roushan, P.; Rubin, N. C.; Sank, D.; Satzinger, K. J.; Smelyanskiy, V.; Strain, D.; Sung, K. J.; Szalay, M.; Takeshita, T. Y.; Vainsencher, A.; White, T.; Wiebe, N.; Yao, Z. J.; Yeh, P.; Zalcman, A. Hartree-Fock on a superconducting qubit quantum computer. *Science* **2020**, *369*, 1084−1089.
(88) Parrish, R. M.; Hohenstein, E. G.; McMahon, P. L.; Martinez, T. J. Quantum Computation of Electronic Transitions Using a Variational Quantum Eigensolver. *Phys. Rev. Lett.* **2019**, *122*, 230401.
(89) Tkachenko, N. V.; Sud, J.; Zhang, Y.; Tretiak, S.; Anisimov, P. M.; Arrasmith, A. T.; Coles, P. J.; Cincio, L.; Dub, P. A. Correlation-Informed Permutation of Qubits for Reducing Ansatz Depth in the Variational Quantum Eigensolver. *PRX Quantum* **2021**, *2*, 020337.
(90) Huggins, W. J.; McClean, J. R.; Rubin, N. C.; Jiang, Z.; Wiebe, N.; Whaley, K. B.; Babbush, R. Efficient and noise resilient measurements for quantum chemistry on near-term quantum computers. *Npj Quantum Inf.* **2021**, *7*, 23.
(91) McClean, J. R.; Rubin, N. C.; Sung, K. J.; Kivlichan, I. D.; Bonet-Monroig, X.; Cao, Y.; Dai, C.; Fried, E. S.; Gidney, C.; Gimby, B.; et al. OpenFermion: The electronic structure package for quantum computers. *Quantum Sci. Technol.* **2020**, *5*, 034014.
(92) Motta, M.; Gujarati, T. P.; Rice, J. E.; Kumar, A.; Masteran, C.; Latone, J. A.; Lee, E.; Valeev, E. F.; Takeshita, T. Y. Quantum simulation of electronic structure with a transcorrelated Hamiltonian:

https://doi.org/10.1021/jacs.4c07670
J. Am. Chem. Soc. XXXX, XXX, XXX−XXX

Improved accuracy with a smaller footprint on the quantum computer. *Phys. Chem. Chem. Phys.* **2020**, *22*, 24270−24281.
(93) Lang, R. A.; Ryabinkin, I. G.; Izmaylov, A. F. Unitary Transformation of the Electronic Hamiltonian with an Exact Quadratic Truncation of the Baker-Campbell-Hausdorff Expansion. *J. Chem. Theory Comput.* **2021**, *17*, 66−78.
(94) Ryabinkin, I. G.; Yen, T.-C.; Genin, S. N.; Izmaylov, A. F. Qubit Coupled Cluster Method: A Systematic Approach to Quantum Chemistry on a Quantum Computer. *J. Chem. Theory Comput.* **2018**, *14*, 6317−6326.
(95) Izmaylov, A. F.; Yen, T.-C.; Lang, R. A.; Verteletskyi, V. Unitary Partitioning Approach to the Measurement Problem in the Variational Quantum Eigensolver Method. *J. Chem. Theory Comput.* **2020**, *16*, 190−195.
(96) Zhang, J. H.; Iyengar, S. S. Graph-$|Q\rangle\langle C|$, a Graph-based Quantum-classical algorithm for efficient electronic structure on hybrid quantum/classical hardware systems: Improved quantum circuit depth performance. *J. Chem. Theory Comput.* **2022**, *18*, 2885.
(97) Iyengar, S. S.; Saha, D.; Dwivedi, A.; Lopez-Ruiz, M. A.; Kumar, A.; Zhang, J. H.; Ricard, T. C.; Richerme, P.; Sabry, A. Quantum Algorithms for the Study of Electronic Structure and Molecular Dynamics: Novel Computational Protocols. In *Comprehensive Computational Chemistry*; Elsevier, 2023.
(98) Lanyon, B. P.; Whitfield, J. D.; Gillett, G. G.; Goggin, M. E.; Almeida, M. P.; Kassal, I.; Biamonte, J. D.; Mohseni, M.; Powell, B. J.; Barbieri, M.; et al. Towards quantum chemistry on a quantum computer. *Nat. Chem.* **2010**, *2*, 106−111.
(99) Lu, D.; Xu, N.; Xu, R.; Chen, H.; Gong, J.; Peng, X.; Du, J. Simulation of chemical isomerization reaction dynamics on a NMR quantum simulator. *Phys. Rev. Lett.* **2011**, *107*, 020501.
(100) Hempel, C.; Maier, C.; Romero, J.; McClean, J.; Monz, T.; Shen, H.; Jurcevic, P.; Lanyon, B. P.; Love, P.; Babbush, R.; Aspuru-Guzik, A.; Blatt, R.; Roos, C. F. Quantum Chemistry Calculations on a Trapped-Ion Quantum Simulator. *Phys. Rev. X* **2018**, *8*, 031022.
(101) GOOGLE AI QUANTUM AND COLLABORATORS; Arute, F.; Arya, K.; Babbush, R.; Bacon, D.; Bardin, J. C.; Barends, R.; Boixo, S.; Broughton, M.; Buckley, B. B.; Buell, D. A.; et al. Hartree-Fock on a superconducting qubit quantum computer. *Science* **2020**, *369*, 1084−1089.
(102) Chia, N.-H.; Chung, K.-M.; Lai, C.-Y. On the Need for Large Quantum Depth. In *Proceedings of the 52nd Annual ACM SIGACT Symposium on Theory of Computing. STOC 2020*; Association for Computing Machinery: New York, NY, USA, 2020; p 902915.
(103) Preskill, J. Quantum Computing in the NISQ era and beyond. *Quantum* **2018**, *2*, 79.
(104) Nelson, E. Feynman Integrals and the Schrödinger Equation. *J. Math. Phys.* **1964**, *5*, 332.
(105) Hastings, M. B. An area law for one-dimensional quantum systems. *J. Stat. Mech.: Theory Exp.* **2007**, *2007*, P08024.
(106) Eisert, J.; Cramer, M.; Plenio, M. B. Colloquium: Area laws for the entanglement entropy. *Rev. Mod. Phys.* **2010**, *82*, 277−306.
(107) Anshu, A.; Harrow, A. W.; Soleimanifar, M. Entanglement spread area law in gapped ground states. *Nat. Phys.* **2022**, *18*, 1362−1366.
(108) Orús, R. A practical introduction to tensor networks: Matrix product states and projected entangled pair states. *Ann. Phys.* **2014**, *349*, 117−158.
(109) Wright, K.; Beck, K. M.; Debnath, S.; Amini, J. M.; Nam, Y.; Grzesiak, N.; Chen, J.-S.; Pisenti, N. C.; Chmielewski, M.; Collins, C.; et al. Benchmarking an 11-qubit quantum computer. *Nat. Commun.* **2019**, *10*, 5464.
(110) Amazon Web Services *Amazon Braket*. 2020; https://aws.amazon.com/braket/.
(111) Moissette, A.; Batonneau, Y.; Brémard, C. Conformation and protonation of 2,2'-bipyridine and 4,4'-bipyridine in acidic aqueous media and acidic ZSM-5 zeolites: A Raman scattering study. *J. Am. Chem. Soc.* **2001**, *123*, 12325−12334.
(112) Vitale, M.; Castagnola, N. B.; Ortins, N. J.; Brooke, J. A.; Vaidyalingam, A.; Dutta, P. K. Intrazeolitic Photochemical Charge Separation for $Ru(bpy)_3^{2+}$ Bipyridinium System: Role of the Zeolite Structure. *J. Phys. Chem. B* **1999**, *103*, 2408−2416.
(113) Graetzel, M. Artificial photosynthesis: Water cleavage into hydrogen and oxygen by visible light. *Acc. Chem. Res.* **1981**, *14*, 376−384.
(114) Howard, S. T. Conformers, Energetics, and Basicity of 2,2'-Bipyridine. *J. Am. Chem. Soc.* **1996**, *118*, 10269−10274.
(115) Steel, P. J. Aromatic nitrogen heterocycles as bridging ligands; a survey. *Coord. Chem. Rev.* **1990**, *106*, 227−265.

https://doi.org/10.1021/jacs.4c07670
J. Am. Chem. Soc. XXXX, XXX, XXX−XXX